

# Measurement of Thermal Parameter using Non-Contact Photopyroelectric Method

Azmi Zakaria,<sup>a\*</sup> Liaw Hock Sang,<sup>b</sup> Zulkifly Abbas,<sup>a</sup> Wan Mahmood Mat Yunus<sup>a</sup> and Jumiah Hassan<sup>a</sup>

<sup>a</sup> Photoacoustic Laboratory, Department of Physics, Universiti Putra Malaysia, 43400 Serdang, Selangor, Malaysia.

<sup>b</sup> College of Engineering, Universiti Tenaga Nasional, 43009 Kajang, Selangor, Malaysia.

\* Corresponding author, E-mail: azmizak@fsas.upm.edu.my

Received 31 Mar 2005

Accepted 22 Aug 2005

**ABSTRACT:** In the standard photopyroelectric technique, a precise control of thermal coupling fluid between the solid sample and the sensor is sometimes difficult, and yet an important factor in sample characterization. In this paper, we propose a non-contact photopyroelectric configuration for thermal diffusivity measurement of solids by considering the phenomena of thermal wave interference. We adopted the thermal wave interferometry, which was extensively discussed by Bennett and Patty in the photoacoustic signal generation, to our photopyroelectric signal generation in a thermally thick condition for a nondestructive testing. A normalization procedure has been used to eliminate a number of media parameters of photopyroelectric cell that otherwise needed to be known before one can determine thermal diffusivity of the sample. The thermal diffusivities obtained for Al, Cu, and Ni samples were close to literature values and thus justified the proposed model.

**KEYWORDS:** photopyroelectric, thermal wave, thermal diffusivity.

## INTRODUCTION

The photopyroelectric (PPE) technique has gained an increasing interest from various areas of applied science and technology, especially in the measurement of thermophysical and optical properties of the materials of either in their single phase of solid<sup>1,2,6</sup>, liquid<sup>2,3,4,6</sup>, gas<sup>3,4,6</sup>, in phase transition<sup>5,6</sup> or combination of them<sup>6</sup>. In the standard PPE technique, a good thermal contact is achieved between the solid sample and the sensor with the coupling fluid, for example the thermal conductive grease, and the quality of PPE signal depends on the precise control of the coupling. However, the thermal coupling fluid containing pores and inhomogeneities make the realization of a well-defined thermal contact difficult. Moreover, the sample may be contaminated by fluid. To overcome these disadvantages, non-contact methods were suggested with the use of gas as the thermal coupling fluid<sup>7,8</sup>.

Several models were proposed for the PPE detection. Antoniow et al<sup>7</sup> developed a two-dimensional model with an axial symmetry and demonstrated the possible detection of thermal wave across an air-gap up to 15 mm. Minamide et al<sup>8</sup> applied the theory of thermal wave propagation suggested by Opsal and

Rosencwaig<sup>9</sup>, in which a thermally inhomogeneous material was modeled with a system of  $N$  plane homogenous layers, to a 3-layer structure consists of graphite, air-gap and polyvinylidene difluoride (PVDF) film. In the contact method by Delenclos et al<sup>10</sup>, a difficult task is involved in solving  $10 \times 10$  matrix by Cramer's rule to obtain the solution for a heat transfer equation in order to reach the final expression for the average PPE voltage. In the normalization procedure, they normalized the liquid sample signal with respect to sensor signal alone, and also to other liquid sample signal.

The PPE technique is well known to be able to reject sound interference from the surrounding and only response to thermal fluctuation. In this paper, we suggest an easy approach of thermal wave interferometry to a non-contact PPE configuration for a nondestructive or non-contact method by applying the theory of thermal wave interference in photoacoustic (PA) signal generation proposed by Bennett and Patty<sup>11</sup>. This approach has greatly reduced the effort to obtain the expression for an average PPE voltage and we will use a normalization procedure to determine the solid sample thermal diffusivity to eliminate a number of media parameters of the PPE cell.

**MATERIALS AND METHODS**

The PPE technique is based on the use of a pyroelectric (PE) transducer to detect the temperature variation caused by a periodic modulated or pulsed optical source in a sample-sensor assembly. The absorption of optical source that is converted into heat initiates rapidly damped traveling thermal wave in a sample. It will be partially reflected and transmitted upon striking at the interface of two media. Generally for a thermal wave propagating in medium 1 towards medium 2, the thermal wave reflection coefficient  $R_{12}$  and the thermal wave transmission coefficient  $T_{12}$  at the interface are respectively given by<sup>11</sup>

$$R_{12} = \frac{1 - b_{12}}{1 + b_{12}}, \quad T_{12} = \frac{2}{1 + b_{12}}, \quad (1)$$

where  $b_{12}$  is the ratio of thermal effusivity of medium 2 to medium 1. In this context, the PE metal electrode coating is neglected to remove the complexity of thermal wave transmission and reflection at PE transducer-coating and air-coating interfaces.

To obtain the expression for complex PPE signal, we add all the transmitted terms of thermal waves transmitted through gas to the rear detection PE detector, instead of that to the front detection microphonic detector in PA technique by Bennett and Patty<sup>11</sup>. If the test sample is highly opaque, in which the optical absorption length is much smaller than sample thickness, this approach is further simplified by considering only heat source generated on the sample surface<sup>12</sup>. Thus, the resulting thermal wave is independent of the optical properties of the sample.

Fig. 1 shows the one-dimensional configuration of the PPE cell with the sample and the air-gap layers in a thermally thin condition, and PE transducer and backing in a thermally thick condition. The first transmitted and the reflected wave at the sample-air interface, respectively, are<sup>11</sup>

$$\theta_{sa1} = T_{sa} A e^{-\sigma_s L_s}, \quad R_{sa1} A e^{-\sigma_s L_s}, \quad (2)$$

where  $A = Q_0 / 2k_s \sigma_s$ ,  $Q_0$  is the source intensity,  $k_j$  is thermal conductivity,  $\sigma_j = (1 + i) / \mu_j$ ,  $\mu_j = \sqrt{\alpha_j / \pi f}$  is the thermal diffusion length at light modulation frequency  $f$ ,  $L_j$  is the thickness,  $\alpha_j = k_j / \rho_j c_j$  is the thermal diffusivity, where  $\rho_j$  is the density, and  $c_j$  is the specific heat of medium  $j$  ( $= s, a, p, b$ ). The reflected wave then will undergo multiple reflections in thermally thin sample between the sample-air interfaces,  $x = -L_a$  and  $x = -(L_a + L_s)$ , and transmissions at  $x = -L_a$ , into air-gap. The transmitted waves to the air-gap, including the first wave  $\theta_{sa1}$ , is

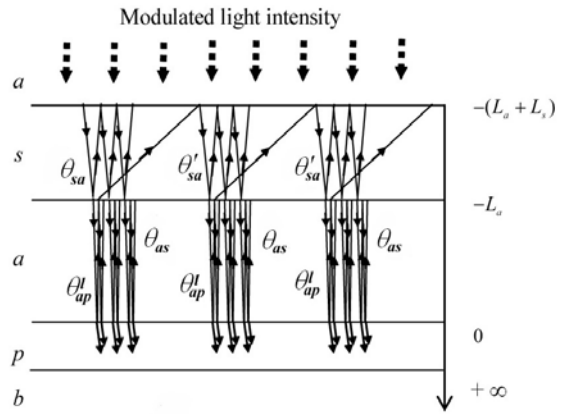


**Fig 1.** One-dimensional configuration of photopyroelectric cell with the route of thermal wave showed;  $s$  is sample,  $a$  is air,  $p$  is PVDF film,  $b$  is backing.

$$\theta_{sa} = \frac{T_{sa} A e^{-\sigma_s L_s}}{1 - R_{sa}^2 e^{-2\sigma_s L_s}} \quad (3)$$

In the air-gap, each transmitted thermal wave will again undergo multiple reflections between the air-sample ( $x = -L_a$ ) and air-PVDF interfaces ( $x = 0$ ), as well as transmissions at the interfaces. The transmitted waves at  $x = 0$  give the first series of transmitted terms to the PVDF film that contributes to its surface temperature,  $\theta_{sa} \theta'_{ap} = \theta_{sa} T_{ap} e^{-\sigma_a L_a} / (1 - R_{sa} R_{ap} e^{-2\sigma_a L_a})$ . The transmitted waves at  $x = -L_a$ , that is  $\theta_{sa} \theta_{as} = \theta_{sa} T_{as} R_{ap} e^{-2\sigma_a L_a} / (1 - R_{ap} R_{as} e^{-2\sigma_a L_a})$ , will undergo multiple reflections in the sample and transmission at  $x = -L_a$ ,  $\theta_{sa} \theta_{as} \theta'_{sa} = \theta_{sa} \theta_{as} R_{sa} T_{sa} e^{-2\sigma_s L_s} / (1 - R_{sa}^2 e^{-2\sigma_s L_s})$ , subsequently, multiple reflections in the air-gap, as well as transmissions at its interfaces. Thus, the transmitted waves at  $x = 0$ ,  $\theta_{sa} \theta_{as} \theta'_{sa} \theta'_{ap}$ , give the second series of

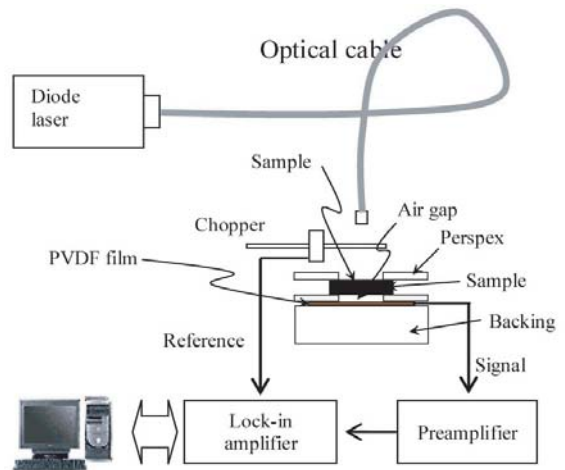


**Fig 2.** Schematic diagram of the experimental setup used for thermal diffusivity measurement.

transmitted terms to the PVDF film. The transmitted waves at  $x = -L_a$  will repeat the above process to give the third series  $\theta_{sa}\theta_{as}\theta_{sa}\theta_{as}\theta_{sa}\theta_{ap}$  and the subsequent series of transmitted terms to the PVDF film infinitely. This is actually an infinite geometric series with ratio  $\theta_{as}\theta_{sa}$ , thus the PVDF surface temperature can be written as

$$\theta_{ap} = \frac{Q_0 T_{ap} T_{sa} e^{-(\sigma_s L_s + \sigma_a L_a)}}{2k_s \sigma_s \left[ (1 - R_{ap} R_{as} e^{-2\sigma_a L_a}) (1 - R_{sa}^2 e^{-2\sigma_s L_s}) - R_{ap} R_{sa} T_{as} T_{sa} e^{-2(\sigma_a L_a + \sigma_s L_s)} \right]} \quad (4)$$

The averaged temperature  $\theta_p$  in the film is

$$\theta_p(\omega) = \frac{\theta_{ap}}{L_p} \int_0^{L_p} e^{-\sigma_p x} dx \quad (5)$$

The average PE voltage  $V(\omega)$  produced by the PVDF film is  $pL_p\theta_p / \epsilon\epsilon_0$ <sup>13</sup>, hence by using expression  $\theta_p$  in eq. (5) the voltage can be written as

$$V(\omega) = \frac{Q_0 T_{ap} T_{sa} p e^{-(\sigma_s L_s + \sigma_a L_a)} (1 - e^{-\sigma_p L_p})}{2\epsilon\epsilon_0 k_s \sigma_s \sigma_p \left[ (1 - R_{ap} R_{as} e^{-2\sigma_a L_a}) (1 - R_{sa}^2 e^{-2\sigma_s L_s}) - R_{ap} R_{sa} T_{as} T_{sa} e^{-2(\sigma_a L_a + \sigma_s L_s)} \right]}, \quad (6)$$

where  $p$  is the PE coefficient,  $\epsilon$  is the dielectric constant of PE detector, and  $\epsilon_0$  is the permittivity constant of vacuum.

For special case that is for the thermally thick condition of sample, we have  $e^{-2\sigma_s L_s} \approx 0$  or  $(1 - R_{sa}^2 e^{-2\sigma_s L_s}) \approx 1$ . Further, normalizing the signal of the test sample to that of the reference sample can eliminate a number of pertinent values for the air and PVDF film. This process also can cancel out the denominator term,  $(1 - R_{ap} R_{as} e^{-2\sigma_a L_a})$ , of the air-gap because the values of the air-to-sample reflection coefficient,  $R_{as}$ , of most metals normally are very close with one another<sup>14</sup>. Therefore, eq. (6) simplifies to

$$\frac{V_s}{V_r}(\omega) = C \frac{e^{-\sigma_s L_s}}{e^{-\sigma_r L_r}},$$

$$= C \exp \left[ -\sqrt{\frac{\pi f}{\alpha_s}} L_s + \sqrt{\frac{\pi f}{\alpha_r}} L_r \right] \times \exp \left\{ i \left[ -\sqrt{\frac{\pi f}{\alpha_s}} L_s + \sqrt{\frac{\pi f}{\alpha_r}} L_r \right] \right\} \quad (7)$$

where  $C = (k_r \sigma_r T_{sa} / k_s \sigma_s T_{ra})$ , and here subscripts  $s$  and  $r$  represent the test and reference samples, respectively. The eq. (7) is similar in form to the one reported by Delenclos et al but with different constant  $C$ <sup>10</sup>. The constant  $C$  is trivial in obtaining the value of thermal diffusivity and that is the reason why we do not consider the sample reflectivity, which is sample dependent and remains constant at single laser wavelength, in our model.

By taking the natural logarithm for the magnitude of eq. (7), the thermal diffusivity of test sample is

$$\alpha_s = \left[ \frac{\sqrt{\pi} L_s}{(\pi L_r^2 / \alpha_r)^{1/2} - m} \right]^2, \quad (8)$$

where  $m$  is the slope from either normalized amplitude plot  $\ln(V_s/V_r)$  versus  $\sqrt{f}$  or normalized phase plot  $(\phi_s - \phi_r)$  versus  $\sqrt{f}$ . Thus, the thermal diffusivity of test sample  $\alpha_s$  can be determined by inserting  $m$ ,  $L_s$ ,  $L_r$ , and  $\alpha_r$  into eq. (8).

Fig. 2 shows the schematic diagram of PPE experimental setup with the layers of the cell illustrated. The intensity of the beam of 450-mW diode laser (B&W TEK Inc. BWF-650-150) is periodically modulated by the variable frequency optical chopper (Stanford Research, SR540) before it illuminates onto the sample surface. About 110 micron-thick air-gap was established between the sample and a 52 micron-thick PVDF film (MSIUSA, DT1-052K/L) by placing a piece of paper, with circular opening at its center. With thermal diffusivity of air of  $0.190 \times 10^{-4} \text{ m}^2/\text{s}$ , the thermal diffusion length in the air is about 450 micron at frequency of 30 Hz, which is very much longer than the air-gap, hence multiple reflections are expected to occur between the air-sample and the air-PVDF film interfaces. The sample, paper and PVDF film together are clamped between two Perspex plates to eliminate the wrap of the PVDF film and the piezoelectric effect of the film, which is due to expansion and contraction of the sample<sup>5</sup>. The output signal from the PE sensor is connected to a low-noise preamplifier (Stanford Research, SR560) and then to a lock-in amplifier (SR530) to isolate the signal from background noise and for signal analysis. The PPE signals of amplitude and phase were recorded simultaneously over the same frequency range that suits the proposed model in theory section for Al ( $L_s = 940$  micron), Cu ( $L_s = 880$  micron) and Ni ( $L_s = 500$  micron) samples at room temperature. Theoretically, the setup can be used in quite a large span of temperature as long as it is not too close to PVDF Curie temperature, 100°C, that will lose PVDF sensitivity and not too close to PVDF embrittlement temperature, -60°C. For each sample, only one thickness was chosen

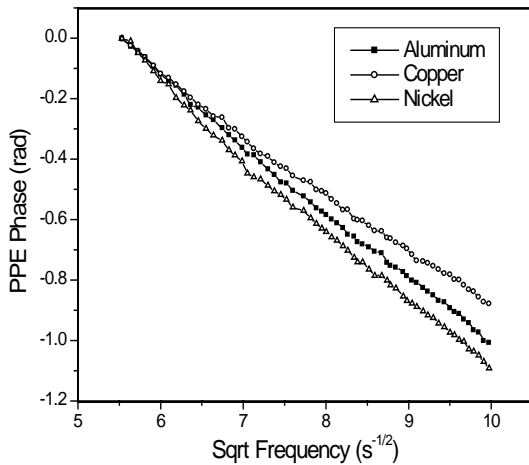


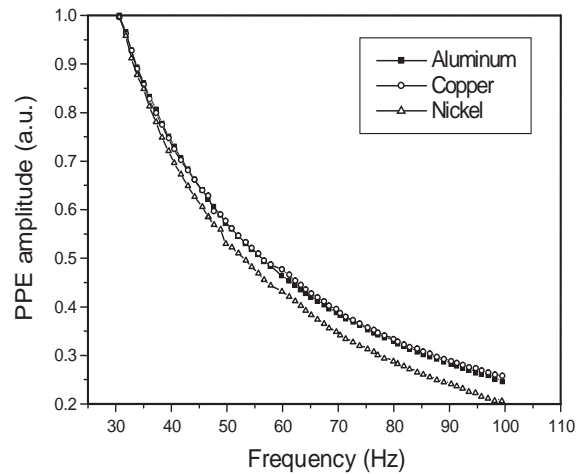
**Fig 3.** The experimental photopyroelectric phase signal versus square root of frequency.

because there should be only a small variation in the thermal diffusivity value expected if several thicknesses of the same sample are tested in one specific region, i.e. in our case of thermally thick region in frequency scanning<sup>12,14</sup>.

Certain practical issues must be tackled in realization of the model. Firstly, the optical absorption length of the sample must be much shorter than its physical thickness at the optical excitation wavelength in order to have the assumption of surface heating fulfilled. For example, it is less than one micron for Al sample for the diode laser wavelength. Otherwise, the studied sample needs to be coated with a thermally very thin layer of material that meets the criteria<sup>12</sup>. Secondly, to eliminate the possibility of the reflected thermal wave from the sample-gas interface contributing significantly to the PPE signal, the modulated frequency is made in such a way that the generated thermal wave in the sample eventually dies off in the sample after a single reflection at the sample-air interface and no reflection in PVDF film. At 30 Hz modulation frequency the PVDF film thermal diffusion length with  $\alpha$  of  $5.4 \times 10^{-8} \text{ m}^2 \text{ s}^{-1}$  is 24 micron, which is shorter than its physical thickness. Thirdly, the difference of term  $\sqrt{\pi/\alpha L}$ 's of the test and of the reference sample in eq. (7) should reasonably and practically be large. Otherwise, it would be close to zero and thus lead to a greater error in calculating the thermal diffusivity.

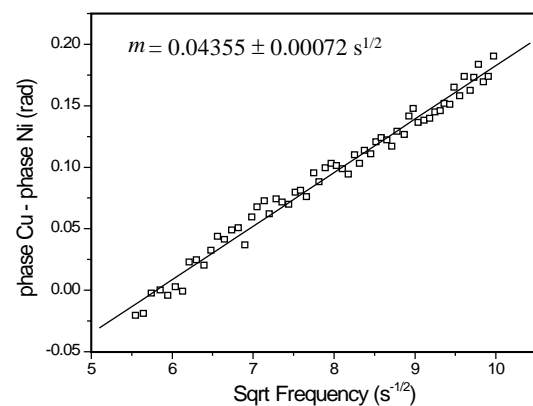
## RESULTS

Fig. 3 shows a linear dependence of PPE phase signal with respect to  $\sqrt{f}$ , for Al, Cu, and Ni samples over modulation frequency range of 30-100 Hz. The thermal diffusion lengths for Al, Cu and Ni are about



**Fig 4.** The experimental photopyroelectric amplitude signal versus frequency.

1020, 1110 and 490 micron, respectively, at 30 Hz; and these lengths decrease as the frequency increases; shortly after this starting frequency the samples will be completely in a thermally thick condition. The plot shows that the Ni sample gives the highest slope among the three samples due to its greatest value of the term  $\sqrt{\pi/\alpha L}$ , as can be interpreted from eq. (7). Fig. 4 shows an exponential decay of PPE amplitude signal with respect to  $f$  of the samples; all signals are normalized to unity. The plot does not show a clear distinct separation between sample Cu and Al curves, as that of the phase signal (Fig. 3), even though both phase and amplitude signals were taken simultaneously. This indicates that the phase evaluation is more sensitive and consistent than that of the amplitude, hence a big error would be expected in calculating thermal diffusivity from the Al amplitude signal in normalization process.



**Fig 5.** The normalized phase signal of copper sample with nickel as reference material.

**Table 1.** Thermal diffusivity obtained using phase signal and comparison with literature value.

Sample	Measured value( $\times 10^{-4}m^2s^{-1}$ )			Average ( $\times 10^{-4} m^2s^{-1}$ )	Literature value ( $\times 10^{-4}m^2s^{-1}$ )	Deviation from literature(%)	Reference
	Al(as reference)	Cu(as reference)	Ni(as reference)				
Al	-	0.942 $\pm$ 0.047	0.978 $\pm$ 0.075	0.960	0.979	1.94	Lide,1997
Cu	1.218 $\pm$ 0.073	-	1.220 $\pm$ 0.104	1.219	1.163	4.82	Lide,1997
Ni	0.230 $\pm$ 0.016	0.222 $\pm$ 0.015	-	0.226	0.230	1.74	Lide,1997

**DISCUSSION**

Fig. 5 shows the plot of the normalized phase signal of Cu with respect to the reference Ni against  $\sqrt{f}$ , and Fig. 6 shows that of normalized amplitude signal of Cu with respect to Ni against  $\sqrt{f}$ . An apparent linear dependence is evident in both graphs over the frequency range of 30-100 Hz and  $m$ 's are the slopes of the linearly fitted lines. The normalized signal is only due to the samples' characteristic, with no influence from the other PPE cell components. The Cu thermal diffusivity, for example, calculated by substituting the literature value of Ni thermal diffusivity is  $1.220 \times 10^{-4} m^2s^{-1}$  when using  $m$  from the normalized phase (Fig. 5), and  $1.198 \times 10^{-4} m^2s^{-1}$  when using  $m$  from normalized amplitude (Fig. 6). The experimental error is only due to errors in the measurement of samples thickness,

$\Delta L \approx 10$  micron, and plot gradient.

Tables 1 and 2 show the calculated thermal diffusivity from the phase and the amplitude signal, respectively, for the samples that were normalized with different reference samples. The thermal diffusivity values obtained from the phase signal are in good agreement within less than 5% from literature values and with the experimental error of less than 8%. The effect of different materials used as references gives about 4% variation in the thermal diffusivity, hence poses no significant change in the value. From the amplitude signal, Table 2, the thermal diffusivity values for Cu and Ni when use each other as reference are in good agreement within 3% with the literature values, and also about 8% experimental error. However for the case of Al, even though the amplitude and the phase signals were recorded simultaneously over the frequency range, the value obtained deviates a lot from the literature value and this may be attributed to the less distinct separation of Al amplitude curve to that of the Cu sample (Fig. 4), such that division during normalization produced a reasonably big error.

In the model, the reflected term from the sample-air interface back into the sample is neglected simply because the modulated frequency is made as such to generate a very short wavelength, and thus short thermal diffusion length, in the sample that dies off after one reflection at the interface. Similarly no reflection is taken into account in the PVDF film because of its short thermal diffusion length as compared to its physical thickness.

In conclusion, we have demonstrated in this paper the potential use of the thermal wave interferometry approach to a non-contact PPE configuration for measuring the thermal diffusivity of solids. The theory

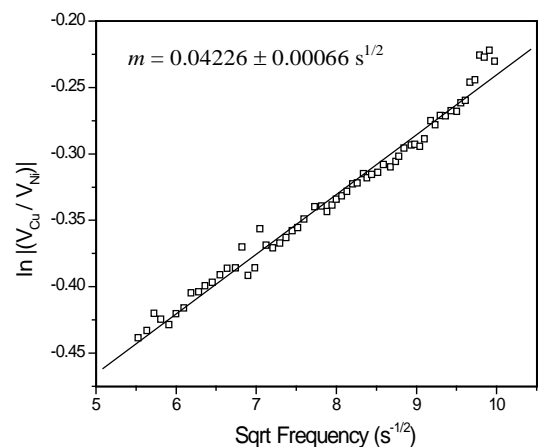


**Fig 6.** The normalized amplitude signal of copper sample with nickel as reference material.

**Table 2.** Thermal diffusivity obtained using amplitude signal and comparison with literature value.

Sample	Measured value( $\times 10^{-4}m^2s^{-1}$ )			Average ( $\times 10^{-4} m^2s^{-1}$ )	Literature value ( $\times 10^{-4}m^2s^{-1}$ )	Deviation from literature(%)	Reference
	Al(as reference)	Cu(as reference)	Ni(as reference)				
Al	-	1.182 $\pm$ 0.063	1.222 $\pm$ 0.103	1.202	0.979	22.8	Lide,1997
Cu	0.953 $\pm$ 0.053	-	1.198 $\pm$ 0.100	1.076	1.163	7.48	Lide,1997
Ni	0.192 $\pm$ 0.013	0.225 $\pm$ 0.015	-	0.209	0.230	9.13	Lide,1997

of thermal wave propagation, suggested by Bennett and Patty, in photoacoustic technique is applicable and has proven to be an easy approach to the PPE technique in a thermally thick condition. The normalization procedure eliminates the need to know a number of pertinent values for other layers of the media in the PPE cell. The obtained values of the thermal diffusivity for aluminum, copper, and nickel samples were close to the literature values, which suggest that the model works well in this condition; the simplicity and sensitivity of the technique suggested that it is a potential candidate for *in situ* non-destructive measurement of the solid thermal diffusivity.

## ACKNOWLEDGEMENTS

The authors are grateful to the Ministry of Science, Technology and the Environment of Malaysia for supporting this work under IRPA Grant No 02-02-04-0132-EA001.

## REFERENCES

- Albuquerque, J E D, Melo, W L B and Faria, R M (2000) Photopyroelectric spectroscopy of polyaniline films. *J Polym Sci Part B: Polym Phys* **38**, 1294-300.
- Pittois, S, Chirtoc, M, Glorieux, C, Bril, W V D and Thoen, J (2001) Direct measurement of thermal conductivity of solids and liquids at very low frequency using the photopyroelectric method. *Analytical Sciences* **17**, s110-s113.
- Shen, J and Mandelis, A (1995). Thermal-wave resonator cavity. *Rev Sc. Instrum* **66**, 4999-5005.
- Lopez, J A B and Mandelis, A (2003) Self-consistent photothermal techniques: Application for measuring thermal diffusivity in vegetable oils. *Rev Sci Instrum* **74**, 700-02.
- Aravind, M and Fung, P C W (1999) Thermal parameter measurements of bulk YBCO superconductor using PVDF transducer. *Meas Sci Technol* **10**, 979-85.
- Bauer, S and Lang, S B (1996) Pyroelectric polymer electrets. *IEEE Trans. on Dielectrics and Electrical Insulation* **3**, 647-76.
- Antoniow, J S, Chirtoc, M and Egee, M (1997) A photopyroelectric method with air as the thermal coupling fluid. *J Phys D: Appl Phys* **30**, 1934-44.
- Minamide, A, Shimaguchi, M and Tokunaga, Y (1998) Study on photopyroelectric signal of optically opaque material measured by polyvinylidene difluoride film sensor. *Jpn J Appl Phys* **37**, 3144-47.
- Opsal, J and Rosencwaig, A (1982) Thermal-wave depth profiling: Theory. *J Appl Phys* **53**, 4240-46.
- Delenclos, S, Chirtoc, M, Sahraoui, A H, Kolinsky, C and Buisine, J M (2001) A new calibration procedure for the determination of thermal parameters and their temperature dependence using the photopyroelectric method. *Analytical Sciences* **17**, s161-s164.
- Bennett, C A and Patty, R R (1982) Thermal wave interferometry: a potential application of the photoacoustic effect. *Appl Optics* **21**, 49-54.
- Marinelli, M, Zammit, U, Mercuri, F and Pizzoferrato, R (1992) High-resolution simultaneous photothermal measurements of thermal parameters at a phase transition with the photopyroelectric technique. *J Appl Phys* **72**, 1096-100.
- Mandelis, A and Zver, M M (1985) Theory of photopyroelectric spectroscopy of solids. *J Appl Phys* **57**, 4421-30.
- Azmi, B Z, Liaw, H S, Yunus, W M M, Hashim, M, Moksini, M M, and Yusoff, W M D W (2004) Normalization procedure in thermal wave approach of thermal diffusivity measurement of solids using pyroelectric sensor. *Infrared Phys & Technol.* **45**, 315-21.
- Lide, R D (1997) *CRC Handbook of Chemistry and Physics 78<sup>th</sup> edition*. CRC Press Inc. Florida.